

Red Supergiant Stars within the Local Group

Lee. R. Patrick



Doctor of Philosophy
The University of Edinburgh
March 2016

Chapter 1

First steps outside the Local Group of Galaxies: Red Supergiants in NGC 55

1.1 Opening remarks

Owen has kindly helped reconstruct and combine the data sets

1.2 Introduction

NGC 55 is a galaxy located outside of the Local Group of Galaxies within the Sculptor Group at a distance of 1.94 ± 0.03 Mpc (Pietrzyński et al., 2006; Gieren et al., 2008) which, before the emergence of the Araucaria Project (Gieren et al., 2005), had been subject to considerable uncertainty (e.g. Pritchett et al., 1987; van de Steene et al., 2006).

The Sculptor Group is considered to be the closest group of galaxies to our own and offers a fantastic laboratory with which to test theories of stellar and galactic evolution as using an 8-m class telescope, one can resolve individual stars within this group. Association to the Sculptor group however, is a contentious issue. Distance estimates vary to each galaxy, but typically when one references this group the main galaxies associated to this reference are: NGC 55, NGC 247,

NGC 253, NGC 300 and NGC 7793. Where NGC 253 is a large starburst galaxy which is the brightest and most dominant galaxy within this group. In addition to these five large spiral galaxies, there are also numerous (~ 20) dwarf galaxies associated to this group.

By revising distances for nine of these dwarfs Karachentsev et al. (2003) postulated that the Sculptor group was actually more like a filament of galaxies, which intersects the Milky Way group, where NGC 55 and NGC 300 and their surrounding satellite galaxies were potentially not associated with the main group of galaxies in this filament. Regardless of the geometry and association to the Sculptor Group, NGC 55 is the nearest large galaxy to the MW group in the direction of the Sculptor Group.

The morphology of NGC 55 is asymmetric and complicated owing to the high inclination angle (up to 80° ; Hummel, Dettmar & Wielebinski, 1986; Westmeier, Koribalski & Braun, 2013). de Vaucouleurs (1961) classified this galaxy as an LMC-like spiral barred galaxy (SB(s)m) where the bar is seen along the line of sight de Vaucouleurs (1961) prompting various claims that this galaxy is an edge on analogue of the LMC (e.g. Robinson & van Damme, 1964, although not cited heavily – two citations in 50 years – the idea has propagated). Figure 1.1 shows NGC 55 and its complicated morphology where one can see the edge-on disk along the major axis of the galaxy and the brighter central part of the galaxy represents the head of the bar. In addition, to NGC 55 being orientated nearly edge on, extending from the disk-bar system there exists many star formation features such as giant H II regions as well as supergiant filaments and shells which are thought to allow ionising radiation to be transported to the halo where star-formation is currently occurring (Ferguson, Wyse & Gallagher, 1996).

The morphology of NGC 55, as well as its known population of massive hot stars (Castro et al., 2008, 2012), points to a recent history of intense star formation. This is supported by the infrared morphology of NGC 55 which is dominated by young star forming features (Engelbracht et al., 2004, with a star formation rate of $0.22 \text{ M}_\odot \text{yr}^{-1}$) as well as indications from near-IR imaging (Davidge, 2005).

The metal content of NGC 55 is expected to be LMC-like, which is supported by Castro et al. (2012) who measured metallicities of 12 blue supergiants using optical spectroscopy and found a mean metallicity $[Z] = -0.40 \pm 0.13 \text{ dex}$. In addition, Webster & Smith (1983) measure abundances of seven H II regions across



Figure 1.1 *Image of NGC 55 where the edge on disk of the galaxy makes up the major axis and the bright central region represents the head of the bar containing intense star forming regions. Image from the Wide Field Imager on the 2.2-metre MPG/ESO telescope at ESO La Silla Observatory. Credit: ESO, press release **Should go the whole hog and bootstrap the RSGs and footprints onto this image ...***

the disk of NGC 55 using the strong-line method (as well as four measurements of the auroral “direct” line method) and found a similar LMC-like metallicity.

Even though the hot massive star population of NGC 55 has been explored, there currently exists no confirmed RSGs in NGC 55, although Davidge (2005) note that the near-IR CMDs of fields within the disk of NGC 55 reveal signatures of RSGs. This study represents the first quantitative study of RSGs in NGC 55 and, by measuring metallicities of this population, will provide a crucial test of the metallicity gradient within this galaxy.

In this chapter I describe the observations undertaken in Section 1.3 and highlight the target selection method and its uncertainties. Section 1.4 details the data reduction process and its complications owing to the poor S/N ratios of the observations. I then present the main results of the chapter in Section 1.5 where I first measure radial velocities for each epoch of the RGSSs, confirming their membership to NGC 55, and then go on to measure stellar parameters for each target using the J -band analysis technique described in detail in Chapter ???. Section 1.6 presents a discussion of the results and the main conclusions are

presented in Section 1.7.

1.3 Observations

The observations for this study were taken using three nights of KMOS guaranteed time observations (GTO) containing xx RSG candidates, the first of which was taken in October 2013 as part of the observations which led to the publication of Gazak et al. (2015). These data consisted of six science exposures (S) of 600s with sky offset exposures (S) interleaved in an O, S, O observing pattern. Seeing conditions for these data were good at $0''.8$ – $1''.2$ throughout the course of the observing block (OB).

The second data set which is made use of in this chapter comes from two nights in September 2014 where the OB used in 2013 was used as backup observations for a programme which required excellent seeing ($<0''.6$). The seeing limits on our observations are more relaxed ($<1''.5$) which gave us an opportunity to make use of some slightly poorer quality KMOS data. On the first night in September 2014 where this OB was observed, the seeing conditions varied widely ($>1''.6$) prompting one observer to comment that “this is the worst recorded seeing at Paranal!”. However, there are 24 science exposures where the seeing conditions were better than $2''.2$, which are (potentially) useful. The final night of observing consisted of 12 exposures with seeing conditions varying between $1''.1$ – $1''.6$.

In addition to the science exposures obtained, on each night a standard set of KMOS calibration files were obtained as well as standard star observations on each night. The standard star observing block for each night is slightly different where in October 2013 HIP 3820 (B8 V; Houk, 1978) was observed using the 24-arm telluric template (KMOS_spec_acq_stdstarscipatt). However, in September 2014 only the three-arm telluric template was observed (KMOS_spec_cal_stdstar), this time with HIP 18926 (B3 V; Houk & Smith-Moore, 1988) and HIP 3820 on both nights.

interestingly both with radial velocity measurements. Could do some nice calibration of the RV measurements? or update their measurements ... remember, we've chosen them to be featureless in this region

Table 1.1 shows the mean measured resolution and resolving power, at the

Table 1.1 Measured velocity resolution and resolving power across each detector.

Date	Det.	IFUs	Ne $\lambda 1.17700 \mu\text{m}$		Ar $\lambda 1.21430 \mu\text{m}$	
			FWHM (km s $^{-1}$)	R	FWHM (km s $^{-1}$)	R
16-10-2013	1	1-8	95.48 \pm 2.46	3140 \pm 81	90.78 \pm 2.12	3302 \pm 77
	2	9-16	88.91 \pm 1.66	3371 \pm 63	86.30 \pm 1.85	3473 \pm 74
	3	17-24	82.96 \pm 2.14	3612 \pm 76	80.77 \pm 2.14	3712 \pm 98
14-09-2015	1	1-8	84.18 \pm 1.93	3561 \pm 82	81.76 \pm 2.15	3667 \pm 96
	2	9-16	87.00 \pm 1.69	3446 \pm 67	84.67 \pm 1.93	3541 \pm 81
	3	17-24	97.14 \pm 1.88	3086 \pm 60	94.85 \pm 2.01	3161 \pm 67
15-09-2014	1	1-8	82.55 \pm 1.96	3632 \pm 86	80.41 \pm 2.30	3728 \pm 106
	2	9-16	88.08 \pm 1.78	3404 \pm 69	86.03 \pm 1.96	3485 \pm 80
	3	17-24	98.04 \pm 1.91	3058 \pm 59	96.74 \pm 2.05	3099 \pm 66

appropriate rotator angles, for each night where the NGC 55 data were taken. This table shows that the resolution can vary significant between each night, particularly on detector three where the mean resolving power changes by a factor of 1/5.

1.3.1 Target Selection

Targets were selected based on the optical photometry from the Araucaria Project (Gieren et al., 2005). The optical CMD which is used to select targets is displayed in Figure 1.2, where the RSG candidates are within the grey box and the observed targets are highlighted in red. This method of target selection was chosen based on the limited extent of near-IR photometry in this area. Figure 1.4 displays the footprints from the Araucaria Project (green) and the ACS Nearby Galaxy Survey Treasury (blue; ANGST Dalcanton et al., 2009) in NGC 55 overlaid on a — image.

The selection criteria employed in this study makes use of the optical $V - I$ colours and m_I magnitudes. Owing to their cool temperatures and extreme luminosities RSGs are known to exist in a “plume” at the tip of a structure of cool stars in the $V - I$, m_I CMD (?) Figure 1.2 displays this CMD and the region of parameter space where RSG candidates reside is marked with a grey box. This box has the limits $17 < m_I < 19$ and $1.2 < V - I < 3.5$ following Gazak et al. (2015). The lower limit of this box are naturally blended in to a population of super-AGB stars which can have luminosities comparable to the faintest RSGs (Nikolaev &

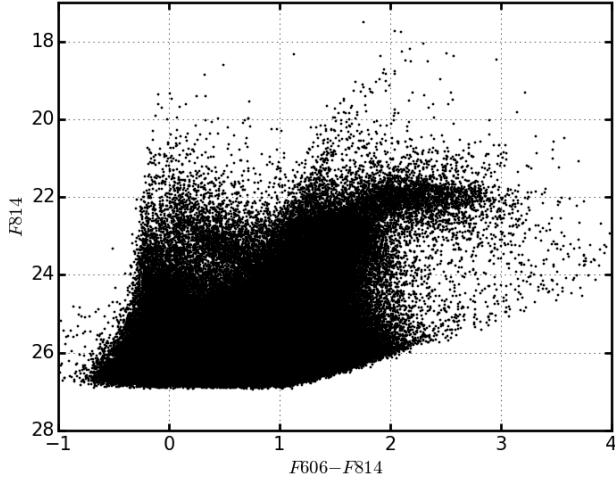


Figure 1.2 Colour magnitude diagram for the NGC 55 optical photometry from the Araucaria Project Gieren et al. (2005). *placeholder! – currently this is from the ANGST data*

Weinberg, 2000, e.g.). However, as stated in Chapter ?? these stars are known to have lifetimes similar to the lowest mass RSGs and arguably still trace the young stellar population of this galaxy.

Table 1.2 shows ground- and space-based optical photometry of the KMOS targets along with their radial velocities (see section 1.5.1).

1.4 Data Reduction

The data reduction was performed with the KMOS/esorex pipeline with a several corrections to improve the quality of the reductions which are fully described and characterised in Turner et al. (in prep).

- Split recombined sky frames into seeing bins
- combine by including pixel shifts between reconstructed IFUs to ensure all frames are correctly matched
- etc.

Would it be useful to use Skycorr to subtract the sky as in Gazak et al. (2015)

Table 1.2 Summary of *VLT-KMOS* targets in *NGC 55*.

ID	S/N	α (J2000)	δ (J2000)	V	I	F606	F814	r_v	(km s $^{-1}$)	Notes
NGC55-RSG19	xx	00:15:29.190	-39:14:08.20	V	17.73	F606	F814	178 ± 7	221 ± 10	195 ± 9
NGC55-RSG20	xx	00:15:29.520	-39:15:13.00	V	18.95	F606	F814	195 ± 17	...	Notes
NGC55-RSG22	xx	00:15:30.520	-39:16:36.70	V	18.56	F606	F814	-17 ± 16	...	Notes
NGC55-RSG24	xx	00:15:31.460	-39:14:46.30	V	18.48	F606	F814	194 ± 6	146 ± 38	Notes
NGC55-RSG25	xx	00:15:31.490	-39:14:32.40	V	18.39	F606	F814	217 ± 15	-341 ± 29	209 ± 12
NGC55-RSG26	xx	00:15:33.160	-39:13:42.00	V	17.96	F606	F814	173 ± 7	...	Notes
NGC55-RSG28	xx	00:15:36.160	-39:15:29.40	V	18.99	F606	F814	161 ± 19	...	Notes
NGC55-RSG30	xx	00:15:38.030	-39:14:50.20	V	18.73	F606	F814	215 ± 9	-423 ± 21	216 ± 12
NGC55-RSG35	xx	00:15:39.260	-39:15:01.70	V	17.87	F606	F814	206 ± 4	223 ± 12	214 ± 3
NGC55-RSG36	xx	00:15:39.520	-39:16:23.10	V	18.46	F606	F814	-284 ± 15	-615 ± 28	194 ± 21
NGC55-RSG39	xx	00:15:40.260	-39:15:01.00	V	17.97	F606	F814	192 ± 5	23 ± 23	187 ± 6
NGC55-RSG43	xx	00:15:40.700	-39:14:50.20	V	18.18	F606	F814	196 ± 5	172 ± 16	193 ± 7
NGC55-RSG46	xx	00:15:41.640	-39:14:58.80	V	18.44	F606	F814	208 ± 12	-128 ± 17	-119 ± 29
NGC55-RSG57	xx	00:15:45.590	-39:15:16.40	V	18.22	F606	F814	197 ± 5	207 ± 13	178 ± 5
NGC55-RSG58	xx	00:15:46.270	-39:15:43.20	V	18.40	F606	F814	216 ± 3	214 ± 21	223 ± 12
NGC55-RSG60	xx	00:15:49.180	-39:17:19.80	V	18.85	F606	F814	26 ± 25	-500 ± 30	349 ± 30
NGC55-RSG65	xx	00:15:51.250	-39:16:26.40	V	17.65	F606	F814	215 ± 3	217 ± 5	204 ± 6
NGC55-RSG67	xx	00:15:53.110	-39:14:13.60	V	18.05	F606	F814	33 ± 21	50 ± 25	28 ± 32
NGC55-RSG69	xx	00:15:55.280	-39:15:00.10	V	18.67	F606	F814	195 ± 8	129 ± 14	202 ± 36
NGC55-RSG70	xx	00:15:56.310	-39:16:08.60	V	18.91	F606	F814	187 ± 8	202 ± 19	184 ± 15
NGC55-RSG71	xx	00:15:56.900	-39:15:27.50	V	18.56	F606	F814	214 ± 10	319 ± 15	256 ± 32
NGC55-RSG73	xx	00:15:57.710	-39:15:41.50	V	18.41	F606	F814	178 ± 5	106 ± 26	182 ± 11

Ground based data from the Araucaria Project Pietrzynski et al. (2006), with typical photometric uncertainty 0.01 and 0.01 in V and I bands respectively. Supplementary ANGST data from Dalcanton et al. (2009), with typical errors 0.015, 0.010, 0.012, in J, H and K bands respectively.

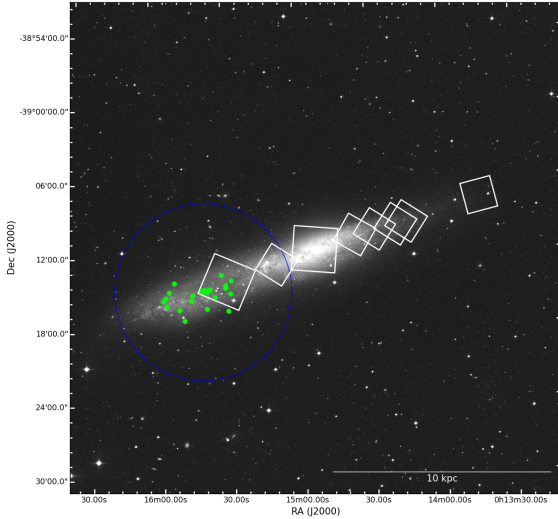


Figure 1.3 Image of NGC 55 with KMOS targets overlaid in green and photometric footprints from the Araucaria Project (Gieren et al., 2005) in xx and the ANGST project (Dalcanton et al., 2009) in white. placeholder! Should do this properly and overlay the regions etc on the pretty eso image.

Telluric correction has been performed by combining and reconstructing the telluric standard exposures using the standard pipeline routines. To improve the performance of the telluric correction I use the method described in detail in Chapter ??.

As mentioned above, were multiple standard star OBs for each night of observing. The telluric spectrum used to correct each science spectrum is determined on a star-by-star basis depending upon a visual inspection of the results of the correction.

1.5 Results

1.5.1 Radial Velocities

Radial velocities are measured using the method described first in Chapter ?. This method is known to work well on KMOS stellar spectra from previous studies Lapenna et al. (2015); Patrick et al. (2015, 2016). Estimated radial velocities from each KMOS pointing is listed in Table 1.2.

Distance modulus = 26.58 ± 0.11 (Tanaka et al., 2011)

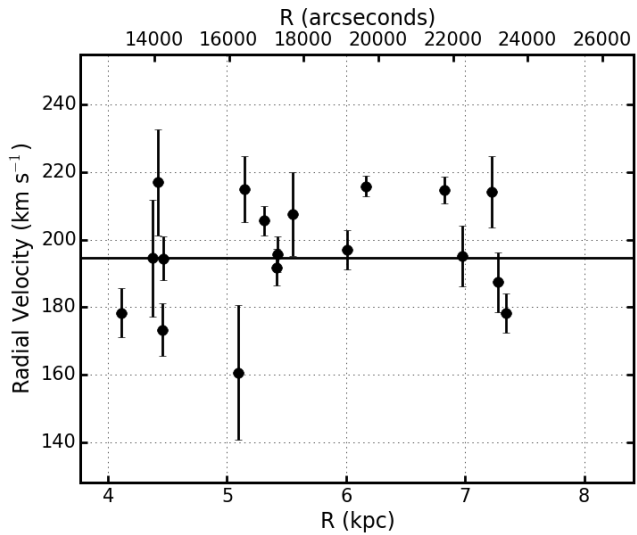


Figure 1.4 Radial velocities for the KMOS RSGs shown against projected radius

- Association with NGC 55
- Does this deserve a subsection of its own?
- Radial velocity Vs. Radius from galaxy centre

1.5.2 Stellar Parameters

- Comparison to previous results
- Z Vs. Radius from galaxy centre
- MCMC parameter estimation for the fit

1.6 Discussion

- Orientation of NGC 55

1.7 Conclusions

Bibliography

- Castro N. et al., 2008, A&A, 485, 41
- Castro N. et al., 2012, A&A, 542, A79
- Dalcanton J. J. et al., 2009, ApJS, 183, 67
- Davidge T. J., 2005, ApJ, 622, 279
- de Vaucouleurs G., 1961, ApJ, 133, 405
- Engelbracht C. W. et al., 2004, ApJS, 154, 248
- Ferguson A. M. N., Wyse R. F. G., Gallagher J. S., 1996, AJ, 112, 2567
- Gazak J. Z. et al., 2015, ApJ, 805, 182
- Gieren W. et al., 2005, The Messenger, 121, 23
- Gieren W., Pietrzyński G., Soszyński I., Bresolin F., Kudritzki R.-P., Storm J., Minniti D., 2008, ApJ, 672, 266
- Houk N., 1978, Michigan catalogue of two-dimensional spectral types for the HD stars
- Houk N., Smith-Moore M., 1988, Michigan Catalogue of Two-dimensional Spectral Types for the HD Stars. Volume 4, Declinations -26deg.0 to -12deg.0.
- Hummel E., Dettmar R.-J., Wielebinski R., 1986, A&A, 166, 97
- Karachentsev I. D. et al., 2003, A&A, 404, 93
- Lapenna E., Origlia L., Mucciarelli A., Lanzoni B., Ferraro F. R., Dalessandro E., Valenti E., Cirasuolo M., 2015, ApJ, 798, 23
- Nikolaev S., Weinberg M. D., 2000, ApJ, 542, 804
- Patrick L. R., Evans C. J., Davies B., Kudritzki R., Hénault-Brunet V., Bastian N., Lapenna E., Bergemann M., 2016, ArXiv e-prints

- Patrick L. R., Evans C. J., Davies B., Kudritzki R.-P., Gazak J. Z., Bergemann M., Plez B., Ferguson A. M. N., 2015, ApJ, 803, 14
- Pietrzynski G. et al., 2006, AJ, 132, 2556
- Pritchett C. J., Schade D., Richer H. B., Crabtree D., Yee H. K. C., 1987, ApJ, 323, 79
- Robinson B. J., van Damme K. J., 1964, in IAU Symposium, Vol. 20, The Galaxy and the Magellanic Clouds, Kerr F. J., ed., p. 276
- Tanaka M., Chiba M., Komiyama Y., Guhathakurta P., Kalirai J. S., 2011, ApJ, 738, 150
- van de Steene G. C., Jacoby G. H., Praet C., Ciardullo R., Dejonghe H., 2006, A&A, 455, 891
- Webster B. L., Smith M. G., 1983, MNRAS, 204, 743
- Westmeier T., Koribalski B. S., Braun R., 2013, MNRAS, 434, 3511